



HAL
open science

Pilot-Induced-Oscillations alleviation through anti-windup based approach

Sophie Tarbouriech, Isabelle Queinnec, Jean-Marc Biannic, Christophe Prieur

► **To cite this version:**

Sophie Tarbouriech, Isabelle Queinnec, Jean-Marc Biannic, Christophe Prieur. Pilot-Induced-Oscillations alleviation through anti-windup based approach. G. Fasano and J. D. Pinter (eds.). Space Engineering Modeling and Optimization with Case Studies, 114, Springer, 2016, Springer Optimization and Its Applications, 978-3-319-41506-2. hal-01393193

HAL Id: hal-01393193

<https://hal.science/hal-01393193>

Submitted on 7 Nov 2016

HAL is a multi-disciplinary open access archive for the deposit and dissemination of scientific research documents, whether they are published or not. The documents may come from teaching and research institutions in France or abroad, or from public or private research centers.

L'archive ouverte pluridisciplinaire **HAL**, est destinée au dépôt et à la diffusion de documents scientifiques de niveau recherche, publiés ou non, émanant des établissements d'enseignement et de recherche français ou étrangers, des laboratoires publics ou privés.

Pilot-Induced-Oscillations alleviation through anti-windup based approach*

Sophie Tarbouriech, Isabelle Queinnec, Jean-Marc Biannic and Christophe Prieur

Abstract The chapter is dedicated to the optimization of a well-known structure of compensators: the anti-windup scheme. This approach belongs to the saturation allowance control class which aims to exploit at the most the actuators capabilities. The objective of this chapter consists of adapting and developing the anti-windup compensator design to some particular classes of nonlinear actuators presenting both magnitude and rate saturations. It is illustrated on the lateral flying case for a civil aircraft in presence of aggressive maneuvering of the pilot. A complete methodology is then proposed comparing several approaches including given anti-PIO filters.

1 Introduction

Control engineers, where possible, like to work under the assumption of linearity. The mathematics associated with the field of linear systems is well developed and underpins much of the control theory which is applied in industry. Even nonlinear techniques often attempt to generalize linear concepts, and frequently nonlinear systems are linearized to obtain linear models which locally yield good engineering approximations [18]. The problem with the assumption of linearity is that it is sometimes unrealistic and can lead to erroneous results. Actually, the increasing re-

S. Tarbouriech - I. Queinnec
LAAS-CNRS, Université de Toulouse, CNRS, Toulouse, France
e-mail: tarbour@laas.fr, queinnec@laas.fr

J.M. Biannic
ONERA, System Control and Flight Dynamics Department, Toulouse, France
e-mail: Jean-Marc.Biannic@onera.fr

C. Prieur
Gipsa-lab, Department of Automatic Control, Grenoble Campus, Saint Martin d'Hères, France
e-mail: christophe.prieur@gipsa-lab.fr

* This work was supported by COCKPIT project, convention ONERA F/20 334/DA PPUJ.

quirements in terms of operational reliability and performance ask to work beyond the linear behavior of the system. Hence, actuators saturations (both magnitude and rate saturations) represent a common nonlinear phenomenon in almost all physical applications, especially in space and aeronautical fields. There are many examples of saturation problems but perhaps the most notorious are those associated with so-called pilot-induced-oscillations (PIO's) in aeronautics (see, for example, [19], [8], [20]). These saturation-induced events have led to the crash of several aircrafts (the SAAB Grippen and the Boeing V22 Osprey are notorious examples [2]) and several near-misses with others. Actually, recall that a pilot-induced oscillation is a sustained or uncontrollable, undesired oscillation resulting from the action of the pilot to control the aircraft. A common nonlinearity leading to PIO is control surface rate limiting. Then this phenomenon can introduce a delayed response and then the action of the pilot implies that the airplane response is essentially opposite of the command wished by the pilot (see, in particular the recent chapter [7]) Thus the presence of saturation can lead to performance degradation from the mild to the severe and can also lead to loss of stability [16], [17]. Although this is not always critical, it is clear that some way of predicting the effects of saturation is required and, moreover, that some method of limiting the degradation that occurs is warranted. This reflects the need for the development of new and more complex control techniques in order to meet the new demands.

In the aeronautical literature, there exist some methods mainly based on the addition of filters or estimators designed to predict and reduce the risk of PIO (see, for example the OLOP criterion using describing functions studied in [12] or the use of a detector based on short time Fourier transform and autoregressive model [21]). In this chapter, we choose another route by considering the use of anti-windup technique, with the objective to provide constructive conditions (that is associating theoretical conditions to optimization routines in order to exhibit effective numerical solutions). More specifically, the approach proposed in this chapter is based on the optimization of a well-known structure of compensators: the anti-windup scheme (see e.g., [26, 32] for an introduction of this notion). This approach belongs to the saturation allowance control class which aims to exploit at the most the actuators capabilities. The basic concept consists of introducing an extra layer to the existing linear controller, accounting for the nonlinearities in order to mitigate the windup phenomenon created by the saturation [15]. This strategy, also called anti-windup design, allows the designer to keep the existing linear controller (already validated) and to introduce a compensator which is active only when the nonlinearity arises. In this framework, numerous works have emerged in the context of both magnitude and rate saturation constraints [25], [6], [10] [13], [11], [30]. Such an approach appears to be really attractive as the anti-windup loop may work with existing control laws (a priori designed by the engineers to answer to defined requirements). Indeed, it represents an interesting technique for the controller designers who can use familiar and intuitive techniques for them and then, simply add an extra layer, which will consider the nonlinear behavior in a second step. If originally, results on anti-windup design consisted on ad-hoc methods intended to work with PID controllers [9], [3], modern anti-windup methods have emerged during the last decade (see, for

example, [31], [14]). Then, the design of such an additional compensator is generally carried out through a static optimization problem of the controller parameters. Thanks to the development of semi-definite programming and convex optimization [5], the anti-windup controller design problem can be formulated as the optimization of a multi-objective criterium (corresponding to closed-loop stability and performance specifications) subject to matrix inequalities constraints associated to the dynamical system. Many different techniques exist in control theory to synthesize such anti-windup controllers, among which static and dynamic linear anti-windup augmentation (see [32]) based on a generalized sector condition representing the saturation [26]. Other anti-windup augmentations are possible as nonlinear synthesis, in particular for control systems equipped with other nonlinearities than magnitude and rate saturations. One can consult [1] for control systems presenting two different sector conditions, and [28] for a control system with a memory-based input.

The objective of this chapter is to adapt and develop the anti-windup compensator design to a class of systems presenting both magnitude and rate saturations. The techniques proposed first include a modeling of the nonlinear actuator involved to further derive analysis and design conditions. It is illustrated on the lateral flying case for a civil aircraft in presence of aggressive maneuvering of the pilot. A complete methodology is then proposed comparing several approaches including given anti-PIO filters (borrowed mainly from [4] and [22]).

The chapter is organized as follows. In Section 2, a complete model of plant, actuator and controller involved to address the stability and performance optimization problem is described. Then, the multi-objective problem to be solved in order to design anti-windup loops is stated. Section 3 pertains to the anti-windup design conditions in two cases depending on the signal used as the input of the anti-windup controller. Then, in order to alleviate the PIO risk for a civil aircraft in presence of aggressive maneuvering of the pilot, Section 4 depicts how the previous techniques are very interesting in comparison with classical anti-PIO filters to guarantee stability and performance of the closed-loop system. Several simulations illustrate the benefits provided by the anti-windup compensators, in terms of simple and systematic methods without needing a tuning parameters step. Finally, some concluding remarks end the chapter.

2 Model description and problem formulation

Anti-windup strategies represent an appropriate framework to mitigate the undesired saturation effects [26], [32]. Thus, the general principle of the anti-windup scheme can be depicted in Figure 1, where the (unconstrained) signal produced by the controller is compared to that which is actually fed into the plant (the constrained signal). This difference is then used to adjust the control strategy by preserving stability and performance.

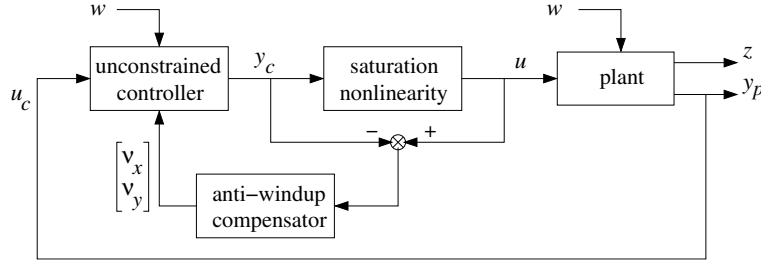


Fig. 1: Principle of anti-windup

The kind of anti-windup controller used in the chapter is specified later and is strongly depending on the considered plant, actuator and controller. Let us first describe the complete model.

Plant model

Unlike most systems in the literature, the outputs of the controller are not affected in a same way by the nonlinear elements. Then, the vector $u \in \mathfrak{R}^m$ building the m inputs of the plant is decomposed into two subvectors: the first one, denoted $u_s \in \mathfrak{R}^{m_s}$, corresponds to m_s saturated inputs, whereas the second one, denoted $u_{ns} \in \mathfrak{R}^{m-m_s}$, corresponds to the linear inputs (unsaturated inputs). The plant model can be defined by:

$$\text{sysP} : \begin{cases} \dot{x}_p = A_p x_p + B_{pu}^s u_s + B_{pu}^{ns} u_{ns} + B_{pw} w \\ y_p = C_p x_p + D_{pu}^s u_s + D_{pu}^{ns} u_{ns} + D_{pw} w \\ z = C_z x_p + D_{zu}^s u_s + D_{zu}^{ns} u_{ns} + D_{zw} w \end{cases} \quad (1)$$

where $x_p \in \mathfrak{R}^{n_p}$ and $y_p \in \mathfrak{R}^p$ are the state and the measured output of the plant. $w \in \mathfrak{R}^q$ generally represents an exogenous perturbation but may also be used to represent a reference signal (or both). Furthermore, $z \in \mathfrak{R}^l$ represents the regulated output, which is used to evaluate the performance of the system with respect to the perturbation w via some pertinent optimization criteria.

Controller model

Differently from the classical anti-windup loops, in which the output of the anti-windup controller is injected to the dynamics of the controller and/or the output of the controller, we consider here that the output of the anti-windup controller modifies only partially the dynamics of the controller and/or the output of the controller. Then, with this in mind, the dynamical controller is described as follows:

$$\text{sysC} : \begin{cases} \dot{x}_c &= A_c x_c + B_c u_c + B_{cw} w + B_{ca} v_x \\ y_{cs} &= C_c^s x_c + D_c^s u_c + D_{cw}^s w + D_{ca} v_y \\ y_{cns} &= C_c^{ns} x_c + D_c^{ns} u_c + D_{cw}^{ns} w \end{cases} \quad (2)$$

where $x_c \in \mathfrak{R}^{n_c}$ and $u_c \in \mathfrak{R}^p$ are the state and the input of the controller. The output of the controller is decomposed into two signals: $y_{cs} \in \mathfrak{R}^{m_s}$, which will be interconnected to u_s through a saturated actuator, and $y_{cns} \in \mathfrak{R}^{m-m_s}$, which will be interconnected with the linear (unsaturated) input u_{ns} . Moreover, v_x and v_y are the additional inputs that will be connected to the anti-windup controller.

B_{ca} and D_{ca} are matrices of dimensions $n_c \times n_{cr}$ and $m_s \times m_r$, and allow to specify what are the n_{cr} states and m_r outputs modified by the anti-windup action.

Actuator model

There is an actuator block between the output of the controller y_c and the input of the plant u , which is decomposed into two blocks: the first one corresponding to the nonlinear (saturated) part and the second one corresponding to the linear (unsaturated) part. The nonlinear actuator part involves n_{dz} nested saturations, including the case of rate and magnitude saturations, as depicted in Figure 2(a). Such nonlinearities will be tackled via the use of dead-zone, denoted $\phi_i(\cdot)$, $i = 1 \dots n_{dz}$.

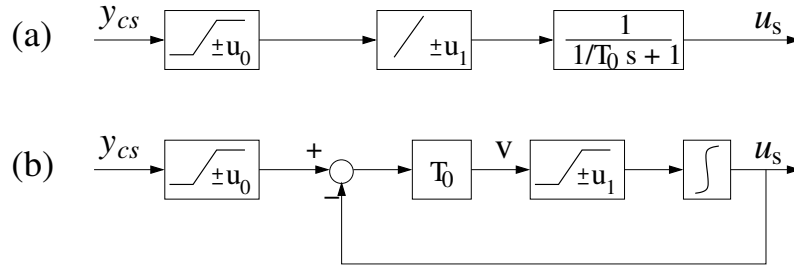


Fig. 2: (a) Actuator with rate and magnitude saturations. (b) Model used to represent such an actuator (scalar case)

The dynamical model of the actuator is based on the scheme 2(b) as follows:

$$\text{sysACT} : \begin{cases} \dot{x}_a = v + \phi_1(v) \\ v = T_0 y_{cs} + T_0 \phi_0(y_{cs}) - T_0 x_a \\ u_s = x_a \end{cases} \quad (3)$$

with $\phi_0(y_{cs}) = \text{sat}_{u_0}(y_{cs}) - y_{cs}$ and $\phi_1(v) = \text{sat}_{u_1}(v) - v$, where $\text{sat}_{u_0}(\cdot)$ and $\text{sat}_{u_1}(\cdot)$ are classical saturation functions and u_0 and u_1 are the levels of saturation in magnitude and in rate, respectively. The elements of the diagonal matrix $T_0 \in \mathfrak{R}^{m_s \times m_s}$ classically take values large enough in order to avoid affecting the linear dynamics of the closed-loop system.

Interconnections

The interconnections considered in the chapter can be described as follows:

- linear link between the output of the plant and the input of the controller: $u_c = y_p$;
- the first part of the output of the controller (y_{cs}) is linked to the corresponding inputs of the plant (u_s) through the actuator model (3);
- the second part of the output of the controller is directly connected to the corresponding inputs of the plant: $u_{ns} = y_{cns}$;
- v_x and v_y are built from the anti-windup compensator (and will be specified later).

Anti-windup compensator

In the DLAW (Direct Linear Anti-Windup) strategy, the anti-windup controller uses as input the difference between the signals issued either from the input and the output of the whole actuator or from the input and the output of the nonlinear elements included in the actuator. Following this, we pursue two strategies to design the anti-windup loops.

- The first strategy is reported in [4] and considers the difference between the input and the output of the actuator defined by $e = u_s - y_{cs} \in \mathfrak{R}^{m_s}$. Additionally, one assumes that the anti-windup controller only acts on the dynamics of the controller, which corresponds to $v_y = 0$, or equivalently, $m_r = 0$. The anti-windup controller of order n_{aw} , with $v_x \in \mathfrak{R}^{n_{cr}}$, reads:

$$AW_e : \begin{cases} \dot{x}_{aw} = A_{aw}x_{aw} + B_{aw}^e(u_s - y_{cs}) \\ v_x = C_{aw}x_{aw} + D_{aw}^e(u_s - y_{cs}) \end{cases} \quad (4)$$

- The second strategy considers that the input of the anti-windup controller are the dead-zones associated to each saturation. Hence, the anti-windup controller of order n_{aw} reads:

$$AW_\phi : \begin{cases} \dot{x}_{aw} = A_{aw}x_{aw} + B_{aw}^0\phi_0(y_c) + B_{aw}^1\phi_1(v) \\ \begin{bmatrix} v_x \\ v_y \end{bmatrix} = C_{aw}x_{aw} + D_{aw}^0\phi_0(y_c) + D_{aw}^1\phi_1(v) \end{cases} \quad (5)$$

where v_x and v_y are of dimensions n_{cr} and m_r , respectively.

Remark 1. The interest of the second anti-windup structure resides in the simplicity of the design conditions. Indeed, the design of a static anti-windup gain (only matrices D_{aw}^0 and D_{aw}^1 are used) is issued from a fully linear problem. In the case of the design of a dynamical anti-windup controller, for a priori given matrices A_{aw} and C_{aw} , the determination of input and transmission matrices is also obtained by solving a linear problem. In the case where $n_{aw} = n_p + n_{m_s} + n_c$, the resolution of a linear problem can also be considered [26]. At the opposite, the first strategy is more adapted to provide analysis conditions but does not allow to simultaneously compute the matrices of the anti-windup and the matrix of the Lyapunov function through a linear optimization problem, even in the static anti-windup case.

Remark 2. The anti-windup model (5) imposes the assumption that the input and output signals of each saturation block is available. To overcome this assumption, alternative strategies can be investigated. For example, the anti-windup may use the difference between the nonlinear actuator and a linear fictitious one (with the same dynamics but without saturation blocks) to explicitly take into account the dynamics of the actuator (present in the rate limiter) [23]. Another option would be to build an observer to evaluate the internal state of the actuator [29]. In these cases, conditions can be derived in a simpler way than that ones issued from the strategy with (4), but they remain more complex than those due to the strategy with (5).

Standard formulation

In [26], a standard formulation of the anti-windup design has been proposed for different kinds of actuators. In the current case, by considering an augmented state of dimensions $n = n_p + m_s + n_c + n_{aw}$ including the state of the plant, the state of the actuator, the state of the controller and the state of the anti-windup controller, the following standard model of the complete closed-loop system can be defined by:

$$\begin{cases} \dot{x} = \mathcal{A}x + \mathcal{B}_0\phi_0(y_c) + \mathcal{B}_1\phi_1(v) + \mathcal{B}_2w \\ y_c = \mathcal{C}_0x + \mathcal{D}_{00}\phi_0(y_c) + \mathcal{D}_{01}\phi_1(v) + \mathcal{D}_{0w}w \\ v = \mathcal{C}_1x + \mathcal{D}_{10}\phi_0(y_c) + \mathcal{D}_{11}\phi_1(v) + \mathcal{D}_{1w}w \\ z = \mathcal{C}_2x + \mathcal{D}_{20}\phi_0(y_c) + \mathcal{D}_{21}\phi_1(v) + \mathcal{D}_{2w}w \end{cases} \quad (6)$$

Then, depending of the anti-windup scheme under consideration, the matrices of the anti-windup controller are encapsulated into the matrices of system (6).

The design procedure of the anti-windup controller consists in optimizing some quantities as the size of the region of stability of the closed-loop system or the guaranteed level of performance. Several optimization problems are then of interest. In particular, the idea by adding the anti-windup loop is to maximize the basin of attraction of the origin for the closed-loop system and/or to minimize the \mathcal{L}_2 gain between w and z or to maximize the set of perturbation w , which can be rejected. Then, throughout the chapter, the signal of perturbation is supposed to be bounded in energy as follows:

$$\|w\|_2^2 = \int_0^\infty w'(t)w(t)dt \leq \delta^{-1}; \quad 0 \leq \delta^{-1} < \infty \quad (7)$$

The problem we intend to address in the chapter can be summarized below.

Problem 1. Determine an anti-windup controller and a region \mathcal{E} , as large as possible, such that

- Internal stability. The closed-loop system (6) with $w = 0$ is asymptotically stable for any initial conditions belonging to \mathcal{E} (which is a region of asymptotic stability (RAS));
- Performance. The \mathcal{L}_2 gain between w and z is finite and equal to $\gamma > 0$.

The convex optimization problems associated to Problem 1 are specified in Sections 3.2 and 3.3.

3 Main Anti-Windup Design Conditions

3.1 Solution to standard anti-windup design

The following proposition provides conditions of local stability and \mathcal{L}_2 performance for the closed-loop system (6). The result regards existence conditions to solve Problem 1.

Proposition 1. *If there exist a symmetric positive definite matrix $Q \in \mathfrak{R}^{n \times n}$, two matrices Z_0 and $Z_1 \in \mathfrak{R}^{m \times n}$, two positive diagonal matrices S_0 and $S_1 \in \mathfrak{R}^{m \times m}$ and a positive scalar γ such that the following conditions are verified:*

$$\begin{bmatrix} Q\mathcal{A}' + \mathcal{A}Q & \mathcal{B}_0S_0 - Q\mathcal{C}'_0 - Z'_0 & \mathcal{B}_1S_1 - Q\mathcal{C}'_1 - Z'_1 & \mathcal{B}_2 & Q\mathcal{C}'_2 \\ \star & -2S_0 - \mathcal{D}_{00}S_0 - S_0\mathcal{D}'_{00} & -\mathcal{D}_{01}S_1 - S_0\mathcal{D}'_{10} & -\mathcal{D}_{0w} & S_0\mathcal{D}'_{20} \\ \star & \star & -2S_1 - \mathcal{D}_{11}S_1 - S_1\mathcal{D}'_{11} & -\mathcal{D}_{1w} & S_1\mathcal{D}'_{21} \\ \star & \star & \star & -I & \mathcal{D}'_{2w} \\ \star & \star & \star & \star & -\gamma I \end{bmatrix} < 0 \quad (8)$$

$$\begin{bmatrix} Q & Z'_{0(i)} \\ \star & \delta u_{0(i)}^2 \end{bmatrix} \geq 0, \quad i = 1, \dots, m \quad (9)$$

$$\begin{bmatrix} Q & Z'_{1(i)} \\ \star & \delta u_{1(i)}^2 \end{bmatrix} \geq 0, \quad i = 1, \dots, m \quad (10)$$

then,

1. when $w = 0$, the set $\mathcal{E}(Q^{-1}, \delta) = \{x \in \mathfrak{R}^n; x'Q^{-1}x \leq \delta^{-1}\}$ is RAS for the closed-loop system (6);
2. when $w \neq 0$, satisfying (7), and for $x(0) = 0$,

- the trajectories of the closed-loop system remain bounded in the set $\mathcal{E}(Q^{-1}, \delta)$;
- the \mathcal{L}_2 gain is finite and one gets:

$$\int_0^T z(t)'z(t) dt \leq \gamma \int_0^T w(t)'w(t) dt, \forall T \geq 0 \quad (11)$$

In an analysis purpose (the anti-windup controller being given), conditions of Proposition 1 are linear and can be directly used to solve adequate optimization problems. Moreover, in the design context, conditions of Proposition 1 are non convex, matrices A_{aw} , B_{aw} , C_{aw} and D_{aw} being hidden in matrices \mathcal{A} , \mathcal{B}_i , \mathcal{C}_i , \mathcal{D}_{ij} , $i, j = 0, 1$. Depending on the problem studied, conditions linear in the decision variables can be obtained, more or less directly, by modifying a bit the original conditions or still by considering iterative procedures (including D-K iteration process) allowing to search for Lyapunov matrix and anti-windup matrices. These situations are detailed in the next subsections.

Remark 3. In the sequel, one considers a set \mathcal{X}_0 , defined by some directions in the plant state space $v_i \in \mathfrak{R}^{n_p}$, $i = 1, \dots, q$, to provide a desired shape of the region $\mathcal{E}(Q^{-1}, \delta)$ to be maximized when solving Problem 1. Then, considering $\bar{v}_i = [v_i' \ 0]'$ $\in \mathfrak{R}^n$, $i = 1, \dots, q$ and β a scaling factor such that $\beta \mathcal{X}_0 \subset \mathcal{E}(Q^{-1}, \delta)$, an additional condition to those of Proposition 1 have to be considered in the algorithms which follow:

$$\begin{bmatrix} \delta \frac{1}{\beta^2} & \delta \bar{v}_i' \\ \delta \bar{v}_i & Q \end{bmatrix} > 0, \quad i = 1, \dots, q \quad (12)$$

3.2 Algorithms for AW_e case

From (1), (2), (3) and (4), matrices of system (6) read:

$$\begin{aligned} \mathcal{A} &= \begin{bmatrix} \mathbb{A} & 0 \\ 0 & 0 \end{bmatrix} + B_{vB}A_{aw}C_{vA} + B_{vB}B_{aw}^e C_{vC} + B_{vD}C_{aw}C_{vA} + B_{vD}D_{aw}^e C_{vC} \\ \mathcal{B}_0 &= \begin{bmatrix} B_{\phi 0} \\ 0 \end{bmatrix}; \quad \mathcal{B}_1 = \begin{bmatrix} B_{\phi 1} \\ 0 \end{bmatrix}; \quad \mathcal{B}_2 = \begin{bmatrix} B_2 \\ 0 \end{bmatrix} + B_{vB}B_{aw}^e C_{vW} + B_{vD}D_{aw}^e D_{0w} \\ \mathcal{C}_0 &= [C_0 \ 0]; \quad \mathcal{C}_1 = [C_1 \ 0]; \quad \mathcal{C}_2 = [C_2 \ 0] \\ \mathcal{D}_{00} &= 0; \quad \mathcal{D}_{01} = 0; \quad \mathcal{D}_{10} = D_1; \quad \mathcal{D}_{11} = 0 \\ \mathcal{D}_{20} &= 0; \quad \mathcal{D}_{21} = 0; \quad \mathcal{D}_{0w} = D_{0w}; \quad \mathcal{D}_{1w} = D_{1w}; \quad \mathcal{D}_{2w} = D_{2w} \end{aligned} \quad (13)$$

with

$$\mathbb{A} = \begin{bmatrix} A_p + B_{pu}^{ns} \Delta^{-1} D_c^{ns} C_p & B_{pu}^s + B_{pu}^{ns} \Delta^{-1} D_c^{ns} D_{pu}^s & B_{pu}^{ns} \Delta^{-1} C_c^{ns} \\ T_0 D_c^s (C_p + D_{pu}^{ns} \Delta^{-1} D_c^{ns} C_p) & T_0 (D_c^s D_{pu}^s - I_{m_s} + D_c^s D_{pu}^{ns} \Delta^{-1} D_c^{ns} D_{pu}^s) & T_0 (C_c^s + D_c^s D_{pu}^{ns} \Delta^{-1} C_c^{ns}) \\ B_c C_p + B_c D_{pu}^{ns} \Delta^{-1} D_c^{ns} C_p & B_c D_{pu}^s + B_c D_{pu}^{ns} \Delta^{-1} D_c^{ns} D_{pu}^s & A_c + B_c D_{pu}^{ns} \Delta^{-1} C_c^{ns} \end{bmatrix}$$

$$B_2 = \begin{bmatrix} B_{pw} + B_{pu}^{ns} \Delta^{-1} (D_c^{ns} D_{pw} + D_{cw}^{ns}) \\ T_0 (D_c^s D_{pw} + D_{cw}^s + D_c^s D_{pu}^{ns} \Delta^{-1} (D_c^{ns} D_{pw} + D_{cw}^{ns})) \\ B_{cw} + B_c D_{pw} + B_c D_{pu}^{ns} \Delta^{-1} (D_c^{ns} D_{pw} + D_{cw}^{ns}) \end{bmatrix}$$

$$B_{\phi 0} = \begin{bmatrix} 0 \\ T_0 \\ 0 \end{bmatrix}; B_{\phi 1} = \begin{bmatrix} 0 \\ I_{m_s} \\ 0 \end{bmatrix}; D_1 = T_0$$

$$C_0 = [D_c^s (I_p + D_{pu}^{ns} \Delta^{-1} D_c^{ns}) C_p \quad D_c^s (I_p + D_{pu}^{ns} \Delta^{-1} D_c^{ns}) D_{pu}^s \quad C_c^s + D_c^s D_{pu}^{ns} \Delta^{-1} C_c^{ns}]$$

$$C_1 = [T_0 D_c^s (I_p + D_{pu}^{ns} \Delta^{-1} D_c^{ns}) C_p \quad T_0 D_c^s (I_p + D_{pu}^{ns} \Delta^{-1} D_c^{ns}) D_{pu}^s - T_0 \quad T_0 (C_c^s + D_c^s D_{pu}^{ns} \Delta^{-1} C_c^{ns})]$$

$$C_2 = [C_z + D_{zu}^{ns} \Delta^{-1} D_c^{ns} C_p \quad D_{zu}^s + D_{zu}^{ns} \Delta^{-1} D_c^{ns} D_{pu}^s \quad D_{zu}^{ns} \Delta^{-1} C_c^{ns}]$$

$$D_{0w} = D_{cw}^s + D_c^s D_{pw} + D_c^s D_{pu}^{ns} \Delta^{-1} (D_c^{ns} D_{pw} + D_{cw}^{ns})$$

$$D_{1w} = T_0 (D_{cw}^s + D_c^s D_{pw} + D_c^s D_{pu}^{ns} \Delta^{-1} (D_c^{ns} D_{pw} + D_{cw}^{ns}))$$

$$D_{2w} = D_{zw} + D_{zu}^{ns} \Delta^{-1} (D_c^{ns} D_{pw} + D_{cw}^{ns})$$

$$B_{vB} = \begin{bmatrix} 0 \\ 0 \\ 0 \\ I_{n_{aw}} \end{bmatrix}; B_{vD} = \begin{bmatrix} 0 \\ 0 \\ B_{ca} \\ 0 \end{bmatrix}; C_{vA} = [0 \ 0 \ 0 \ I_{n_{aw}}]$$

$$C_{vC} = [-D_c^s (I_p + D_{pu}^{ns} \Delta^{-1} D_c^{ns}) C_p \quad I_m - D_c^s (I_p + D_{pu}^{ns} \Delta^{-1} D_c^{ns}) D_{pu}^s \quad -C_c^s - D_c^s D_{pu}^{ns} \Delta^{-1} C_c^{ns} \quad 0]$$

and $\Delta = I_{m-ms} - D_c^{ns} D_{pu}^{ns}$.

In the analysis context, conditions of Proposition 1 using the AW_e structure are linear in the decision variables and can be directly used. On the other hand, in the design context, conditions of Proposition 1 are nonlinear due to, in particular, the products between the Lyapunov matrix Q and the matrices of the anti-windup controller. Then, to address the design and solve Problem 1, some iterative procedure can be applied by considering at the first step a given static ($n_{aw} = 0$) or dynamic ($n_{aw} \neq 0$) anti-windup controller.

The following algorithms can be used.

Algorithm 3.1 Analysis of a given AW_e anti-windup controller

1. Give matrices A_{aw} , B_{aw}^e , C_{aw} and D_{aw}^e .
2. Choose directions to be optimized $v_i \in \mathfrak{R}^{n_p}$, $i = 1, \dots, q$ and a known perturbation with bound δ .
3. Solve

$$\min_{Q, S_0, S_1, Z_0, Z_1, \gamma, \mu} \gamma + \mu$$

subject to LMI (8), (9), (10) and (12)

where γ is the \mathcal{L}_2 gain between w and z and $\mu = 1/\beta^2$.

Algorithm 3.2 Design of a AW_e anti-windup controller

1. Select an initial guess for matrices A_{aw} , B_{aw}^e , C_{aw} and D_{aw}^e of appropriate dimensions in order to build the desired anti-windup loop. A static anti-windup AW_e may also be used by considering $n_{aw} = 0$.
2. Choose directions to be optimized $v_i \in \mathfrak{R}^{n_p}$, $i = 1, \dots, q$ and a known perturbation with bound δ .
3. Analysis step – Solve

$$\min_{Q, S_0, S_1, Z_0, Z_1, \gamma, \mu} \gamma + \mu$$

subject to LMI (8), (9), (10) and (12)

where γ is the \mathcal{L}_2 gain between w and z and $\mu = 1/\beta^2$.

4. If the solution obtained is satisfactory (some accuracy has to be fixed) or no more improved from the previous steps then STOP. Otherwise, go to the next iteration (the idea is to finish by an analysis step).
5. Synthesis step – Pick the solution Q obtained at Step 3 and solve

$$\min_{A_{aw}, B_{aw}^e, C_{aw}, D_{aw}^e, S_0, S_1, Z_0, Z_1, \gamma} \gamma$$

subject to LMI (8), (9), (10) and (12)

6. Go to Step 3.

Remark 4. The selection of an initial guess of anti-windup in the Algorithm 3.2 must take care of the dimension of each elements but must also verify that A_{aw} is Hurwitz. Actually, it is not possible to initialize the problem with null matrices of appropriate dimensions (for a given order of the anti-windup scheme n_{aw}) as the condition on \mathcal{A} in the first block of inequality (8) imposes that both the closed-loop linear dynamics of the system and the anti-windup dynamics are asymptotically stable. An option may then be to select any stable dynamical matrix A_{aw} with matrices B_{aw}^e , C_{aw} and D_{aw}^e equal to null matrices of appropriate dimensions. This initial anti-windup scheme is ineffective but allows to solve the analysis step and obtain a matrix Q to be used in the synthesis step.

3.3 Algorithms for AW_ϕ case

As for the previous case, from (1), (2), (3) and (5), matrices of system (6) are defined by:

$$\begin{aligned} \mathcal{A} &= \begin{bmatrix} \mathbb{A} & B_v C_{aw} \\ 0 & A_{aw} \end{bmatrix}; \mathcal{B}_0 = \begin{bmatrix} B_{\phi 0} + B_v D_{aw}^0 \\ B_{aw}^0 \end{bmatrix}; \mathcal{B}_1 = \begin{bmatrix} B_{\phi 1} + B_v D_{aw}^1 \\ B_{aw}^1 \end{bmatrix} \\ \mathcal{C}_0 &= [C_0 \ C_{v0} C_{aw}]; \mathcal{C}_1 = [C_1 \ C_{v1} C_{aw}]; \mathcal{C}_2 = [C_2 \ 0] \\ \mathcal{D}_{00} &= C_{v0} D_{aw}^0; \mathcal{D}_{01} = C_{v0} D_{aw}^1; \mathcal{D}_{10} = D_1 + C_{v1} D_{aw}^0; \mathcal{D}_{11} = C_{v1} D_{aw}^1 \\ \mathcal{B}_2 &= \begin{bmatrix} B_2 \\ 0 \end{bmatrix}; \mathcal{D}_{20} = 0; \mathcal{D}_{21} = 0; \end{aligned} \quad (14)$$

Matrices \mathbb{A} , B_2 , $B_{\phi 0}$, $B_{\phi 1}$, D_1 , C_0 , C_1 , C_2 , \mathcal{D}_{0w} , \mathcal{D}_{1w} and \mathcal{D}_{2w} remain unchanged. Matrices defining the interconnection between the anti-windup loop and the system are:

$$B_v = \begin{bmatrix} 0 \\ T_0 D_{ca} [0 \ I_{m_r}] \\ B_{ca} [I_{n_{cr}} \ 0] \end{bmatrix}; C_{v0} = D_{ca} [0 \ I_{m_r}]; C_{v1} = T_0 D_{ca} [0 \ I_{m_r}]$$

As in the previous case, the analysis problem (Algorithm 3.3) is linear and the synthesis problem of the anti-windup is nonlinear, including products between decision variables, and in particular between the Lyapunov matrix Q and the anti-windup elements. As for the AW_e strategy, a D-K iteration procedure may then be considered for the synthesis problem (Algorithm 3.4). However, differently for the AW_e strategy, the synthesis optimization problem may be partially linearized and, for given matrices A_{aw} and C_{aw} , the design of matrices B_{aw}^i and D_{aw}^i , $i = 0, 1$ can be handled via a linear optimization problem (Algorithm 3.5).

Algorithm 3.3 *Analysis of a given AW_ϕ anti-windup controller*

1. Select matrices A_{aw} , B_{aw}^0 , B_{aw}^1 , C_{aw} , D_{aw}^0 and D_{aw}^1 .
2. Choose directions to be optimized $v_i \in \mathfrak{R}^{n_p}$, $i = 1, \dots, q$ and a known perturbation with the bound δ .
3. Solve

$$\begin{aligned} &\min_{Q, S_0, S_1, Z_0, Z_1, \gamma, \mu} \gamma + \mu \\ &\text{subject to LMI (8), (9), (10) and (12)} \end{aligned}$$

where γ is the \mathcal{L}_2 gain between w and z and $\mu = 1/\beta^2$.

Algorithm 3.4 *Design of a AW_ϕ anti-windup controller*

1. Select matrices A_{aw} , B_{aw}^0 , B_{aw}^1 , C_{aw} , D_{aw}^0 and D_{aw}^1 of appropriate dimensions in order to build the desired anti-windup loop. A static anti-windup AW_ϕ may also be used by considering $n_{aw} = 0$.
2. Choose directions to be optimized $v_i \in \mathfrak{R}^{n_p}$, $i = 1, \dots, q$ and a known perturbation with bound δ .
3. Analysis step – Solve

$$\min_{Q, S_0, S_1, Z_0, Z_1, \gamma, \mu} \gamma + \mu$$

subject to LMI (8), (9), (10) and (12)

where γ is the \mathcal{L}_2 gain between w and z and $\mu = 1/\beta^2$.

4. If the solution obtained is satisfactory (some accuracy has to be fixed) or no more improved from the previous steps then STOP. Otherwise, go to the next iteration (the idea is to finish by an analysis step).
5. Synthesis step – Pick the solution Q obtained at Step 3 and solve

$$\min_{S_0, S_1, Z_0, Z_1, B_{aw}^0, B_{aw}^1, D_{aw}^0, D_{aw}^1, \gamma} \gamma$$

subject to LMI (8), (9), (10) and (12)

6. Go to Step 3.

Algorithm 3.5 Design of a AW_ϕ anti-windup controller with fixed dynamics

1. Give matrices A_{aw} and C_{aw} .
2. Choose directions to be optimized $v_i \in \mathfrak{R}^{n_p}$, $i = 1, \dots, q$ and a known perturbation with the bound δ .
3. Solve

$$\min_{Q, S_0, S_1, Z_0, Z_1, \bar{B}_{aw}^0, \bar{B}_{aw}^1, \bar{D}_{aw}^0, \bar{D}_{aw}^1, \gamma, \mu} \gamma + \mu$$

subject to LMI (8), (9), (10) and (12)

where γ is the \mathcal{L}_2 gain between w and z and $\mu = 1/\beta^2$.

4. Compute $B_{aw}^0 = \bar{B}_{aw}^0 S_0^{-1}$, $B_{aw}^1 = \bar{B}_{aw}^1 S_1^{-1}$, $D_{aw}^0 = \bar{D}_{aw}^0 S_0^{-1}$ and $D_{aw}^1 = \bar{D}_{aw}^1 S_1^{-1}$.

Remark 5. In Algorithm 3.5, condition (8) is not directly applied. The products between B_{aw}^i and D_{aw}^i with the matrices S_i are replaced by the change of variables \bar{B}_{aw}^i and \bar{D}_{aw}^i , $i = 0, 1$, which allows to linearize the problem.

Remark 6. An interesting case is the static anti-windup one, for which matrices A_{aw} and C_{aw} are null matrices of appropriate dimensions. It implies that B_{aw}^i , $i = 0, 1$ are also null matrices of appropriate dimensions and only matrices D_{aw}^i , $i = 0, 1$ are computed in the linear Algorithm 3.5.

Remark 7. Matrices A_{aw} and C_{aw} to be used in Algorithm 3.5 may be selected as the solution of a full-order ($n_{aw} = n_p + n_c + m_s$) anti-windup compensator design where

the actuator is just a saturation in magnitude (see, for example, the conditions provided in [26]), i.e. via a linear optimization problem. Eventually, an order-reduction step may also be considered in order to select matrices A_{aw} and C_{aw} (see Example 8.5 in [26]). Other procedures developed in [32] could be used.

4 Anti-windup and its use for PIO alleviation

The design and analysis algorithms of Section 3 are now applied and compared in the realistic context of lateral maneuvers of a civil transport aircraft. A specific attention will be devoted to aggressive pilot's demands in conjunction with actuator loss.

In the following, the pilot's activity is modeled as a static gain K_{pil} . For this application, a normal activity would correspond to $K_{pil} = 1$. But, in stressful situations, notably in case of actuators loss, a more aggressive pilot's behavior is generally observed, resulting in much higher gains. Here, the gain is set to $K_{pil} = 3$.

4.1 Problem setup and objectives

The two anti-windup structures AW_e and AW_ϕ above described are compared in this applicative part of the chapter. Both nonlinear closed-loop Simulink implementations are sketched in Figures 3 and 4, respectively. For each design strategy, the state-space models $sysP$ and $sysC$ are readily obtained from the Simulink diagrams of Figures 3 and 4 with the help of the Matlab `linmod` function. The plant corresponds to the "yellow box" depicting the aircraft system while the global controller (including pilot actions) is obtained by extraction of the 3 blue boxes. A standard balanced reduction technique is finally applied to obtain reasonably sized models. The obtained reduced orders, respectively $n_p = 8$ and $n_c = 20$, are compatible with the proposed algorithms. The aircraft system involves 2 inputs ($m = 2$) with only the ailerons deflection actuator which saturates ($m_s = 1$), and 5 outputs ($p = 5$), among which the performance output which is set as the roll angle ($l = 1$). The disturbance of the system is due to the saturation of the input, i.e., $B_{pw} = B_{pu}^s$ ($q = 1$).

In the AW_e strategy, the anti-windup input is a single scalar signal ($m_s = 1$) which only captures the difference between the input of the nonlinear ailerons deflection actuator and its output. In the AW_ϕ strategy, two signals (one for the magnitude limitation and one for the rate limitation) are used by the anti-windup device. Their generation is detailed in the Simulink implementation of Figure 5.

Whatever the considered approach, both anti-windup controllers act similarly on the internal dynamics of the nominal lateral controller of the aircraft through two scalar signals v_p and v_b which respectively affect roll and sideslip angles dynamics ($v_x = [v_p \ v_b]'$ and $v_y = 0$, $n_{cr} = 2$, $m_r = 0$). Remark yet that the second strategy offers more flexibility with the possibility of a direct anti-windup action at the controller

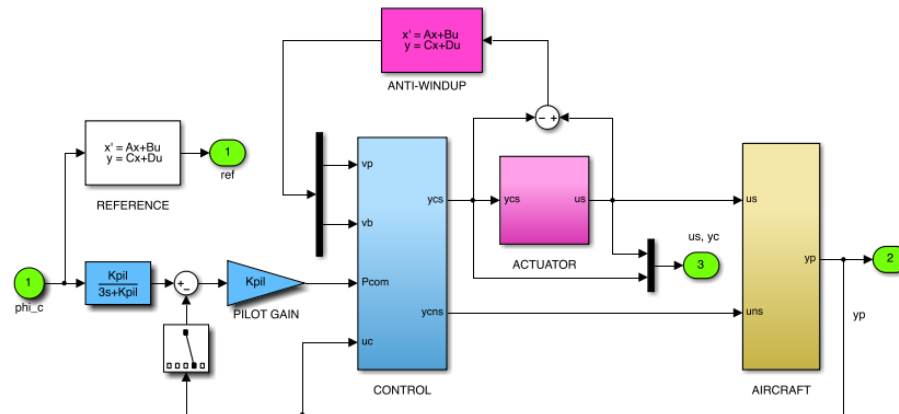


Fig. 3: Nonlinear closed-loop Simulink implementation of Anti-Windup AWe for lateral aircraft simulations

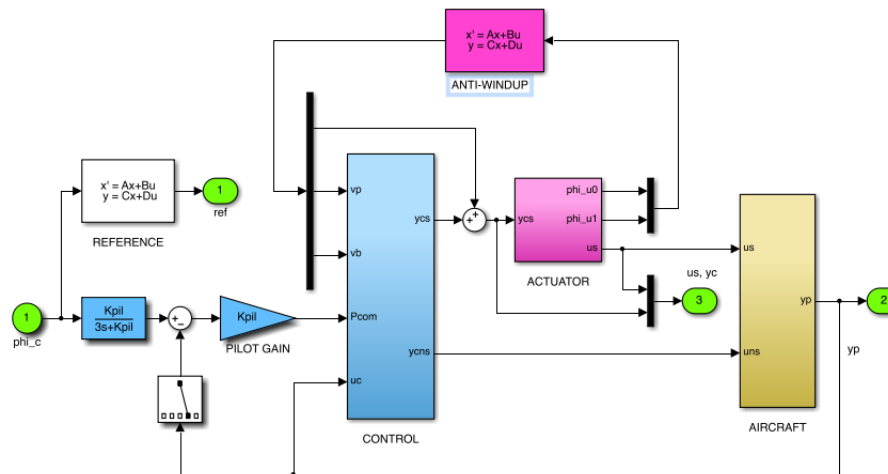


Fig. 4: Nonlinear closed-loop Simulink implementation of Anti-Windup AW_ϕ for lateral aircraft simulations

output. However, no significant improvement has been observed with this additional feature which has thus not been further considered in this application.

The main objective of this application is to design and evaluate anti-windup systems to improve the aircraft response to roll angle solicitations while limiting oscillations despite actuator loss [22]. During such maneuvers, a significant control activity is observed on the ailerons. This is why the effects of saturations are mod-

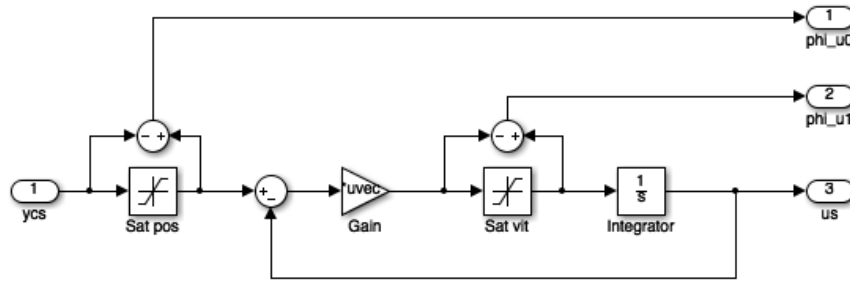


Fig. 5: Detailed view of the magnitude and rate limitations system

eled and taken into account for these actuators in both diagrams of Figures 3 and 4 while no saturation is introduced on the rudders. The effects of saturations become even more penalizing in case of a partial loss of control capability. Assume indeed that the aircraft is controlled by a pair of ailerons on each wing but only one is operational. In that case, the activity of the remaining actuators is doubled as well as the risk of magnitude and rate saturations. Then, the magnitude and rate limits in the following will be halved. We will consider $L_m = 10deg$ (instead of 20 in normal conditions) and $L_r = 20deg/s$ (instead of 40).

In the sequel, five different anti-windup compensators are implemented and compared:

- A standard anti-PIO filter used in the industry. It is an "open-loop" solution which does not exploit the information relative to the saturation of the signal (see [4]). This may be considered as the basic solution from the industry. It corresponds to the block REFERENCE in Figures 3 and 4;
- A dynamic $\mathcal{H}_\infty AW_e$ anti-windup built by using a structured \mathcal{H}_∞ design method [22]. The advantage of such a strategy is that it circumvents some limitations of LMI-based strategies (limitation on the size problem when manipulating LMIs, conservatism of sufficient conditions) but to the detriment of the easiness of construction for engineers not always specialists of advanced control theories;
- A dynamic AW_e anti-windup designed with the Algorithm 3.2 initialized with the $\mathcal{H}_\infty AW_e$ anti-windup above-described;
- A dynamic AW_ϕ anti-windup designed with the Algorithm 3.5 using matrices A_{aw} and C_{aw} borrowed to the $\mathcal{H}_\infty AW_e$ anti-windup;
- A static AW_ϕ anti-windup designed with the Algorithm 3.5. This strategy is an alternative to the standard anti-PIO filter as it is very easy to implement (no additional dynamical system to introduce in the controller block).

4.2 Analysis and design of anti-windup AW_e

First, an analysis step (in terms of stability and performance) of the anti-windup controller proposed in [4] (denoted $\mathcal{H}_\infty AW_e$ anti-windup) is carried out. This anti-windup compensator has been built by using a structured \mathcal{H}_∞ design method [22]. Such an anti-windup has provided very good numerical results but no proof of its stability in closed-loop was a priori ensured. By using Algorithm 3.1, one can verify that the conditions are feasible. The optimization problem is then solved by considering the bound on perturbation $\delta = 0.1$ and $v_1 = [C_p(4, :) \ 0]$ as the direction to be optimized over the set $\mathcal{L}(Q^{-1}, \delta)$. Algorithm 3.1 gives the optimal solution:

$$\text{Analysis } \mathcal{H}_\infty AW_e : \gamma = 1.7167 ; \beta = 0.6254$$

It is interesting to do the same analysis for the closed-loop system without anti-windup. The feasibility is also obtained and the solution is:

$$\text{Analysis without anti-widup: } \gamma = 1.8929 ; \beta = 0.7851$$

The solution with the $\mathcal{H}_\infty AW_e$ anti-windup described through γ and β as performance indicators does not appear as much better than the one without anti-windup: indeed γ is actually decreased in the case with anti-windup but β is slightly degraded. However, simulations presented in [4] exhibited that the time responses with the $\mathcal{H}_\infty AW_e$ strategy were very close to the desired behavior (that is without saturation), differently from the case without anti-windup resulting in large overshoot and degraded time evolution. The meaning of this is that the considered criterion of optimization, which does not explicitly include the time response performance, does not exactly fit to the analysis or design of the anti-windup loop. Nevertheless, considering criteria on time response performance is a difficult task and the optimization criterion used here gives a reasonable trade-off between stability guarantee, performance and time response.

In a second step, Algorithm 3.2 is used by considering the previous anti-windup controller at the initialization step (Step 1). After one iteration (after the conditions become unfeasible for numerical reasons), one gets a new anti-windup controller AW_e such that:

$$\text{Design } AW_e : \gamma = 1.6887 ; \beta = 0.6978$$

Now, we compare the results obtained in response to a step demand of 40 deg on the roll angle, by using the scheme given in Figure 3.

In Figure 6, the time evolutions obtained with the $\mathcal{H}_\infty AW_e$ anti-windup (used in the first step of analysis) and the AW_e anti-windup above designed are compared. The case without saturation is also plotted (denoted "reference" in the figure). The time evolution of inputs δ_{pc} is plotted in both cases and without saturation in Figure 7.

Remark 8. Note that the level of performance obtained with the $\mathcal{H}_\infty AW_e$ anti-windup cannot be much improved with our strategy as this "initial" anti-windup had been

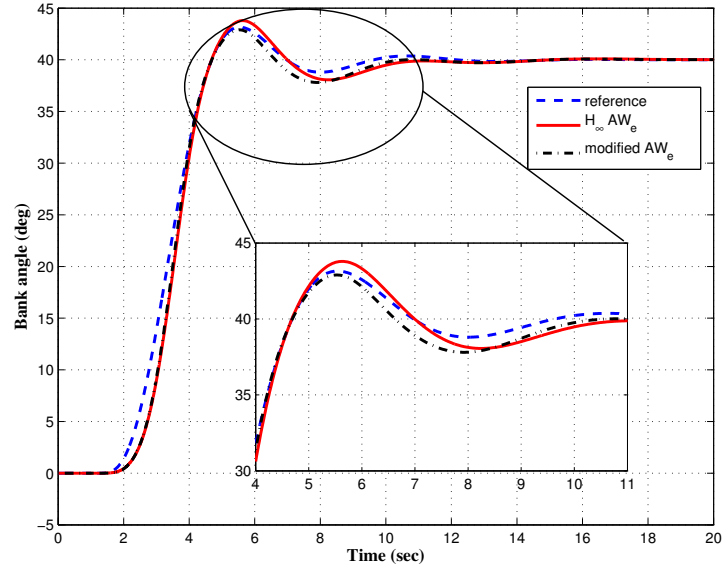


Fig. 6: Roll solicitation of 40 deg: comparison of the performance outputs for the cases with $\mathcal{H}_\infty AW_e$ anti-windup and designed anti-windup AW_e

cleverly designed with the structured \mathcal{H}_∞ approach. The iterative procedure could be initialized with any other anti-windup controller of order n_{aw} , for example (as suggested before) solution of a design in the case of magnitude saturation only. The initial choice has however a significant influence on the iterative process and the attainable solution. Many tests have shown that the results obtained are often not much convincing (generally the solution extended from the initial $\mathcal{H}_\infty AW_e$ anti-windup shows better performance indexes) and then it seems that this anti-windup structure is not much adapted to a design from scratch.

4.3 Design of anti-windup AW_ϕ

In this section, we consider the second strategy, whose main advantage is that it is based on a systematic method without tuning parameter. Figure 4 shows how the AW_ϕ anti-windup is implemented.

As commented in Section 3, in the context of the AW_ϕ strategy, the design of matrices B_{aw}^i and D_{aw}^i is cast by solving a linear optimization problem. Then, for the same conditions on δ and \mathcal{X}_0 as in the previous case, and by considering matrices A_{aw} and B_{aw} of the $\mathcal{H}_\infty AW_e$ anti-windup, Algorithm 3.5 gives matrices B_{aw}^i and D_{aw}^i ,

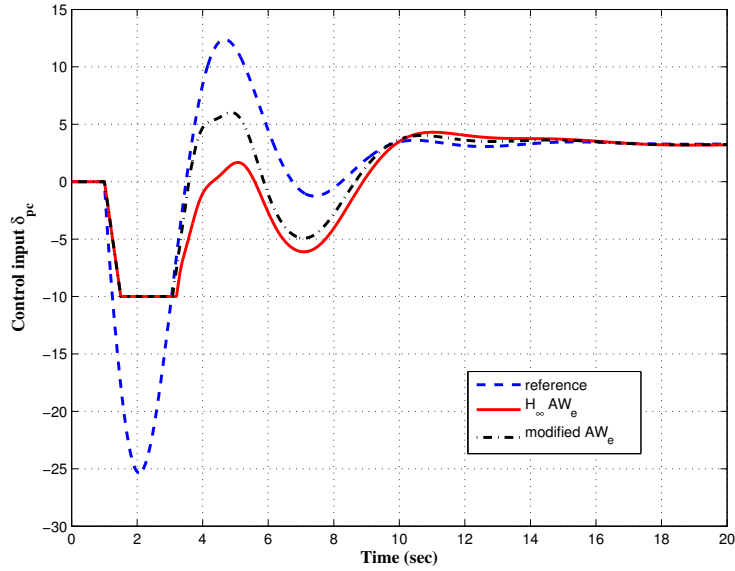


Fig. 7: Roll solicitation of 40 deg: comparison of the inputs for the cases with $\mathcal{H}_\infty AW_e$ anti-windup and designed anti-windup AW_e

$i = 0, 1$, and the following optimal solution

$$\text{Design of dynamical } AW_\phi : \gamma = 1.8441 ; \beta = 0.9013$$

As previously, we consider a Roll solicitation of 40 deg to compare the results. The time responses of the roll angle for the case without saturation, with the $\mathcal{H}_\infty AW_e$ anti-windup and the designed dynamic AW_ϕ anti-windup are plotted in Figure 8. Similarly, the time evolutions of δ_{pc} in these cases are depicted in Figure 9.

One can observe that the level of performance of the $\mathcal{H}_\infty AW_e$ anti-windup is slightly degraded in the case of the design of AW_ϕ , but it remains acceptable.

Now, we design a static AW_ϕ anti-windup (only matrices D_{aw}^i , $i = 0, 1$, have to be designed). The main advantage is that we do not need to initialize the algorithm as matrices A_{aw} and C_{aw} do not exist ($n_{aw} = 0$). Algorithm 3.5 provides the following optimal solution:

$$\text{Static } AW_\phi \text{ design} : \gamma = 1.7846 ; \beta = 0.7772$$

Figures 10 and 11 illustrate the time evolution of the closed-loop system to a roll solicitation of 40 deg. The responses are compared by considering the case without saturation, a standard anti-PIO strategy (see [4]) and the static AW_ϕ anti-windup strategy. It is important to underline that a simple static anti-windup strategy allows

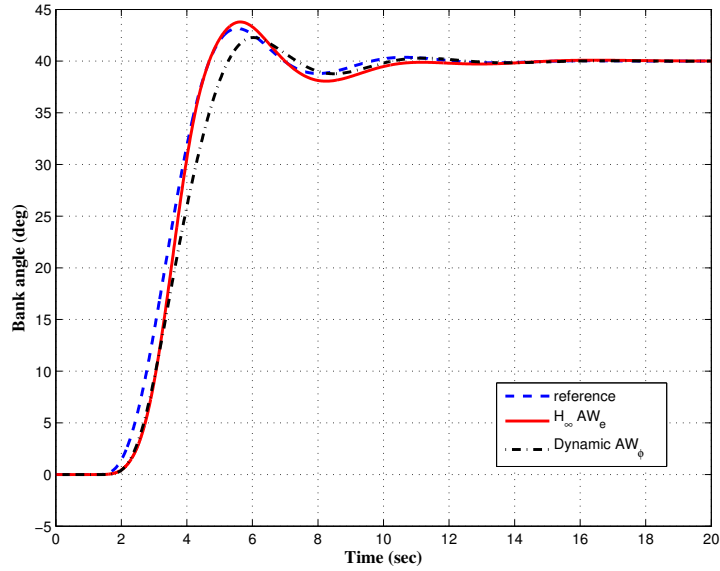


Fig. 8: Roll solicitation of 40 deg: comparison of the performance outputs for the cases with $\mathcal{H}_\infty AW_e$ anti-windup and designed anti-windup AW_ϕ

to obtain better performance than the standard anti-PIO case, which adds dynamics in the system.

5 Conclusion

In this chapter, an anti-windup analysis and design strategy has been proposed for systems involving both magnitude and rate saturations, and taking into consideration that such saturations elements only affect some of the inputs. Such a situation has much practical interest for many systems issued in particular from aerospace domain. It is illustrated here on a lateral flying model of a civil aircraft in presence of aggressive maneuvering of the pilot. Actually magnitude and rate saturations of the ailerons deflection actuator may lead to an undesirable behavior which is often called Pilot-Induced-Oscillation (PIO). For this class of nonlinear control systems, anti-windup compensators have been adapted through adequate convex optimization schemes. A comparison with given dynamic anti-PIO filters already used for this class of systems has also been provided. This work lets many questions open, such as the design of other anti-windup schemes. Other classes of fruitful anti-windup compensators may include the parameter-varying approach [24] or reset controllers [27].

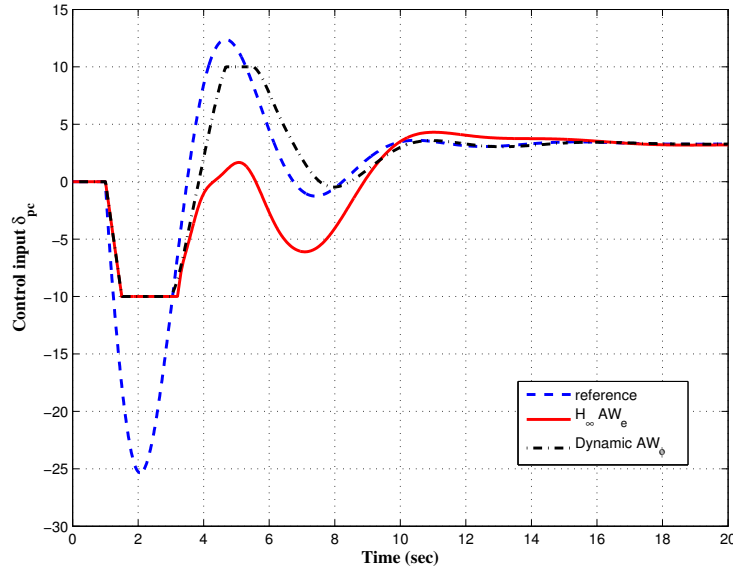


Fig. 9: Roll solicitation of 40 deg: comparison of the inputs for the cases with $\mathcal{H}_\infty AW_e$ anti-windup and designed anti-windup AW_ϕ

References

1. V. Andrieu, C. Prieur, S. Tarbouriech, and D. Arzelier. Global asymptotic stabilization of systems satisfying two different sector conditions. *Systems & Control Letters*, 60(8):570–578, 2011.
2. anon. Why the gripen crashed. *Aerospace America*, 32(2):11, 1994.
3. K. J. Åström and L. Rundqwist. Integrator windup and how to avoid it. In *American Control Conference*, pages 1693–1698, Pittsburgh, PA, 1989.
4. J.-M. Biannic and S. Tarbouriech. Analyse et ajustement de lois de commande en présence de saturations implantation de filtres anti-PIO générés par synthèse anti-windup. Technical report, Rapport COCKPIT/OCKF/CO1.1, 2011.
5. S. Boyd and S.P. Vandenberghe. *Convex optimization*. Cambridge University Press, 2004.
6. O. Brieger, M. Kerr, D. Leissling, I. Postlethwaite, J. Sofrony, and M.C. Turner. Anti-windup compensation of rate saturation in an experimental aircraft. In *American Control Conference*, pages 924–929, New York, 2007.
7. R. D’Andrea, M. Wyss, and M. Waibel. *Challenges Actuated Wingsuit for Controlled, Self-Propelled Flight*, volume The Impact of Control Technology, 2nd Edition, T. Samad and A.M. Annaswamy (eds.). IEEE-CSS, 2014.
8. H. Duda. Prediction of pilot-in-the-loop oscillations due to rate saturation. *Journal of Guidance, Control and Dynamics*, 20(3):581–587, 1997.
9. H. A. Fertik and C. W. Ross. Direct digital control algorithm with anti-windup feature. *ISA Transactions*, 6:317–328, 1967.
10. S. Galeani, S. Onori, A.R. Teel, and L. Zaccarian. A magnitude and rate saturation model and its use in the solution of a static anti-windup problem. *Systems & Control Letters*, 57(1):1–9, 2008.

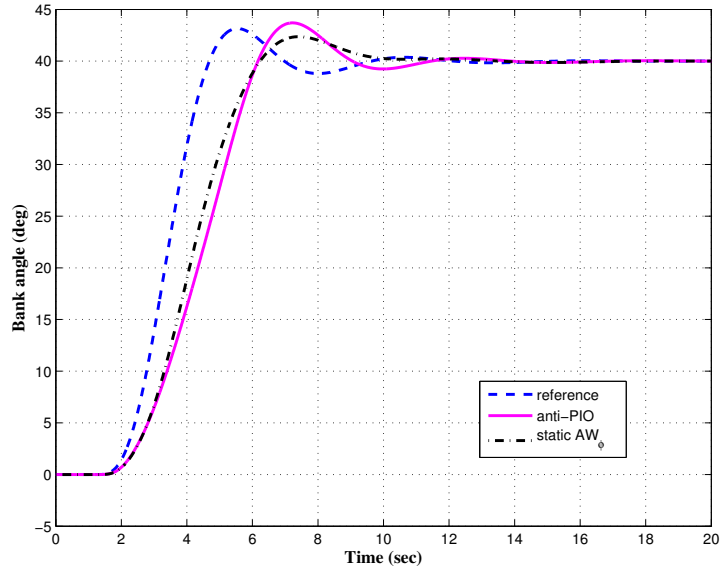


Fig. 10: Roll solicitation of 40 deg: comparison of the performance outputs for the cases with standard anti-PIO and static anti-windup AW_ϕ

11. S. Galeani, S. Tarbouriech, M.C. Turner, and L. Zaccarian. A tutorial on modern anti-windup design. *European Journal of Control*, 15(3-4):418–440, 2009.
12. G.P. Gilbreath. *Prediction of PIO due to actuator rate limiting using the open-loop onset point (OLOP) criterion*. Msc thesis, Dep. of Aeronautics and Astronautics, AirForce Institute of Technology, Ohio, USA, 2001.
13. A.H. Glattfelder and W. Schaufelberger. *Control systems with input and output constraints*. Springer-Verlag, London, 2003.
14. G. Grimm, J. Hatfield, I. Postlethwaite A.R., Teel, M.C. Turner, and L. Zaccarian. Anti-windup for stable linear systems with input saturation: an LMI based synthesis. *IEEE Transactions on Automatic Control*, 48(9):1509–1525, 2003.
15. P. Hippe. *Windup in control. Its effects and their prevention*. AIC, Springer, Germany, 2006.
16. T. Hu and Z. Lin. *Control systems with actuator saturation: Analysis and design*. Birkhäuser, Boston, 2001.
17. V. Kapila and K. Grigoriadis (Eds.). *Actuator saturation control*. Marcel Dekker, Inc., 2002.
18. H.K. Khalil. *Nonlinear systems*. MacMillan, 1992.
19. D.H. Klyde, D.T. McRuer, and T.T. Myers. Pilot-induced oscillation analysis and prediction with actuator rate limiting. *Journal of Guidance, Control and Dynamics*, 20(1):81–89, 1997.
20. D.H. Klyde, N. Richards, and B. Cogan. Use of active inceptor cueing to mitigate pilot-vehicle system loss of control. In *AIAA Guidance, Navigation, and Control Conference*, Minneapolis, USA, August 2012.
21. Q. Liu. *Pilot-induced-oscillation detection and mitigation*. PhD thesis, Cranfield University, 2012.
22. G. Puyou, J.-M. Biannic, and J. Boada-Bauxell. Application of robust antiwindup design to the longitudinal aircraft control to cover actuator loss. In *19th IFAC Symposium on Automatic Control in Aerospace*, University of Wurzburg, Germany, September 2013.
23. I. Queinnec, S. Tarbouriech, and G. Garcia. Anti-windup design for aircraft control. In *IEEE Conference on Control Applications (CCA)*, Munich, Germany, 2006.

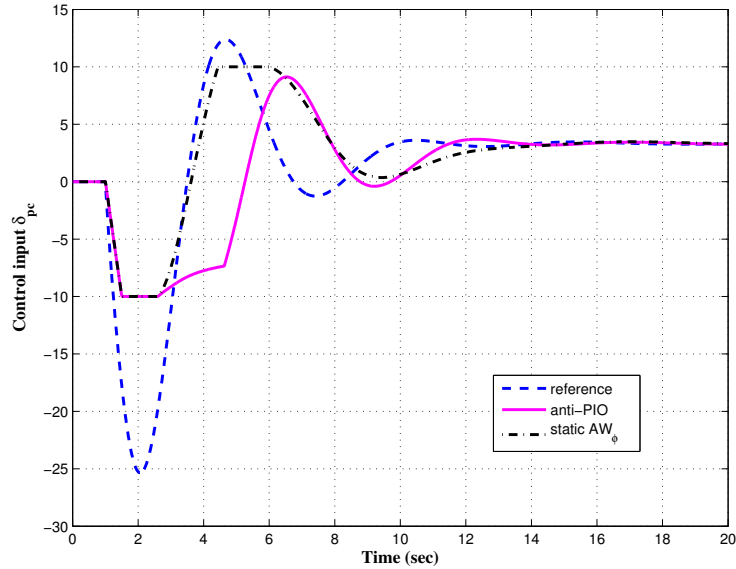


Fig. 11: Roll solicitation of 40 deg : comparison of the inputs for the cases with standard anti-PIO and static anti-windup AW_ϕ

24. C. Roos, J-M. Biannic, S. Tarbouriech, C. Prieur, and M. Jeanneau. On-ground aircraft control design using a parameter-varying anti-windup approach. *Aerospace Science and Technology*, 14(7):459–471, 2010.
25. L. Rundquist and K. Stahl-Gunnarsson. Phase compensation of rate-limiters in unstable aircraft. In *IEEE Conference on Control Applications*, 1996.
26. S. Tarbouriech, G. Garcia, J. M. Gomes da Silva Jr., and I. Queinnec. *Stability and Stabilization of Linear Systems with Saturating Actuators*. Springer, 2011.
27. S. Tarbouriech, T. Loquen, and C. Prieur. Anti-windup strategy for reset control systems. *International Journal of Robust and Nonlinear Control*, 21(10):1159–1177, 2011.
28. S. Tarbouriech, I. Queinnec, and C. Prieur. Stability analysis and stabilization of systems with input backlash. *IEEE Transactions on Automatic Control*, 59(2):488–494, 2014.
29. S. Tarbouriech, I. Queinnec, and M.C. Turner. Anti-windup design with rate and magnitude actuator and sensor saturations. In *European Control Conference*, Budapest, Hungary, 2009.
30. S. Tarbouriech and M.C. Turner. Anti-windup design: an overview of some recent advances and open problems. *IET Control Theory and Application*, 3(1):1–19, 2009.
31. A.R. Teel. Anti-windup for exponentially unstable linear systems. *International Journal of Robust and Nonlinear Control*, 9:701–716, 1999.
32. L. Zaccarian and A.R. Teel. *Modern anti-windup synthesis*. Princeton University Press, 2011.